



Colloidal synthesis of zincblende $\text{Cu}_3\text{InZnSnS}_6$ nanocrystals and their optical property



Zhaomin Hao^a, Zhe Zhang^c, Wei Liu^c, Xu Du^c, Yi Ji^c, Yong Cui^{b,c,*}

^a Henan Key Laboratory of Polyoxometalate Chemistry, College of Chemistry and Chemical Engineering, Henan University, China

^b Institute of Metal Research, Chinese Academy of Sciences, Division of Materials for Special Environments, China

^c Renewable Bioproducts Institute, Georgia Institute of Technology, USA

ARTICLE INFO

Article history:

Received 28 April 2015

Received in revised form

14 May 2015

Accepted 15 May 2015

Available online 23 May 2015

Keywords:

$\text{Cu}_3\text{InZnSnS}_6$

Nanoparticles

Solar energy material

UV–vis

ABSTRACT

Multinary metal sulfides semiconductor nanocrystals have received great attention for their application in solar cells. In this work, we have successfully synthesized the $\text{Cu}_3\text{InZnSnS}_6$ nanocrystals via a colloidal way. The $\text{Cu}_3\text{InZnSnS}_6$ nanocrystals were characterized by X-ray powder diffraction, energy dispersive X-ray spectrometry, transmission electron microscopy and UV–vis spectrometry. The $\text{Cu}_3\text{InZnSnS}_6$ nanocrystals possess metastable zincblende structure, stoichiometric composition and good dispersed property in organic solvent. The bandgap of $\text{Cu}_3\text{InZnSnS}_6$ nanocrystals calculated from UV–vis spectrometry is 1.44 eV, which is the optimal bandgap for photovoltaic absorber, and it displays a potential application in the field of thin film solar cells.

© 2015 Elsevier B.V. All rights reserved.

1. Introduction

Semiconductor materials possess excellent optical and electrical properties that can be applied in many fields, such as photocatalysis [1], solar cells [2], light emitting diode [3] etc. Recently, multinary chalcogenide semiconductor materials have received lots of interests due to their outstanding properties with direct band gap and high absorption coefficient [4]. CuInS_2 , Cu_2SnS_3 and $\text{Cu}_2\text{ZnSnS}_4$, as the representatives, have attracted wide attention [5]. It is well known that CuInS_2 , Cu_2SnS_3 and $\text{Cu}_2\text{ZnSnS}_4$ possess three phase, stable tetragonal structure, metastable zincblende and wurtzite structures. The metastable zincblende and wurtzite phase of CuInS_2 , Cu_2SnS_3 and $\text{Cu}_2\text{ZnSnS}_4$ can be viewed as being derived from zincblende and wurtzite structure of ZnS [6], where Zn^{2+} cations are differently substituted of Cu^+ , In^{3+} , Zn^{2+} , Sn^{4+} . As known, during the process of nanocrystals synthesis, the obtained nanocrystals' structure is often different because of the distinction of reaction conditions. Chemical reaction parameters, such as temperature, solvent, and capping agents, play an important role to the product of crystalline phase. Up to now, a series of nanocrystals have been successfully synthesized by adjusting the reactivity of precursors and bonding strength of ligands [7–11].

The metastable CuInS_2 [12], Cu_2SnS_3 [13] and $\text{Cu}_2\text{ZnSnS}_4$ [14] have synthesized by a colloidal approach. However, the metastable zincblende structure $\text{Cu}_3\text{InZnSnS}_6$ has not been reported. The $\text{Cu}_3\text{InZnSnS}_6$ compound could be regarded as the sequential cation cross-substitutions product from binary II–VI (ZnS) semiconductors, and also can be viewed as the combination of ternary I–III–VI₂ (CuInS_2) and quaternary I₂–II–IV–VI₄ ($\text{Cu}_2\text{ZnSnS}_4$) chalcogenides. There are five different kinds of elements in the same compound and the reactivity of precursors is widely different, so it is hard to synthesize the $\text{Cu}_3\text{InZnSnS}_6$ nanocrystals. Herein, $\text{Cu}_3\text{InZnSnS}_6$ colloidal nanocrystals have been successfully synthesized via a hot injection method for the first time. Oleylamine and Oleylamine/sulfur were employed as capping ligands to balance the reactivity of metal precursors and sulfur source, respectively. By investigating the UV–vis of as-synthesized $\text{Cu}_3\text{InZnSnS}_6$ colloidal nanocrystals, the suitable bandgap of $\text{Cu}_3\text{InZnSnS}_6$ colloidal nanocrystals indicate that they can be applied in the field of thin film solar cells.

2. Experimental details

2.1. Chemicals

CuCl , $\text{InCl}_3 \cdot 4\text{H}_2\text{O}$, oleylamine (OLA, 80–90%), SnCl_4 , $\text{Zn}(\text{CH}_3\text{COO})_2$, sulfur powder were purchased from Aladdin Inc. All chemicals were used as received without further purification.

* Corresponding author at: Institute of Metal Research, Chinese Academy of Sciences, Division of Materials for Special Environments, China.

E-mail address: excellentcui@hotmail.com (Y. Cui).

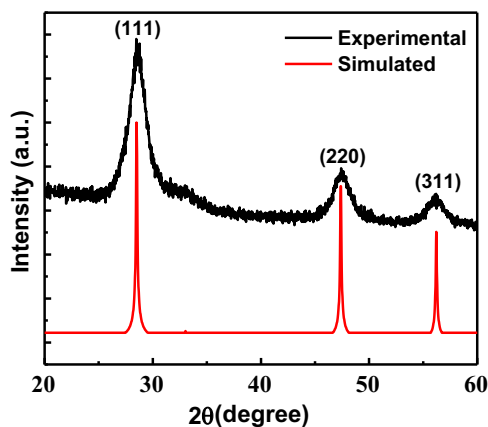


Fig. 1. XRD patterns of $\text{Cu}_3\text{InZnSnS}_6$ nanocrystals with zincblende structure.

2.2. Synthesis of zincblende $\text{Cu}_3\text{InZnSnS}_6$ nanocrystals

0.3 mmol CuCl , 0.1 mmol $\text{InCl}_3 \cdot 4\text{H}_2\text{O}$, 0.1 mmol $\text{Zn}(\text{CH}_3\text{COO})_2$, 0.1 mmol SnCl_4 , 10 mL oleylamine were added to a 25 mL three-neck flask and the reaction mixture was heated to 120 °C. The inside of the flask was degassed by a vacuum pump for 10 min and argon gas was changed from the balloon. This procedure was repeated three times to remove the oxygen and water. When the temperature was increased to 240 °C, 1 mL sulfur/oleylamine (1 mmol/mL)[13] was swiftly injected into the solution under vigorously magnetic stirring. The color of the solution turned black immediately. Then the reaction was kept at 240 °C for 30 min. After the reaction, the crude solution was cooled to 60 °C and then precipitated with 30 mL ethanol and further isolated by centrifugation and decantation. The purified nanocrystals were re-dispersed in toluene or chloroform for detail characterization without size selection.

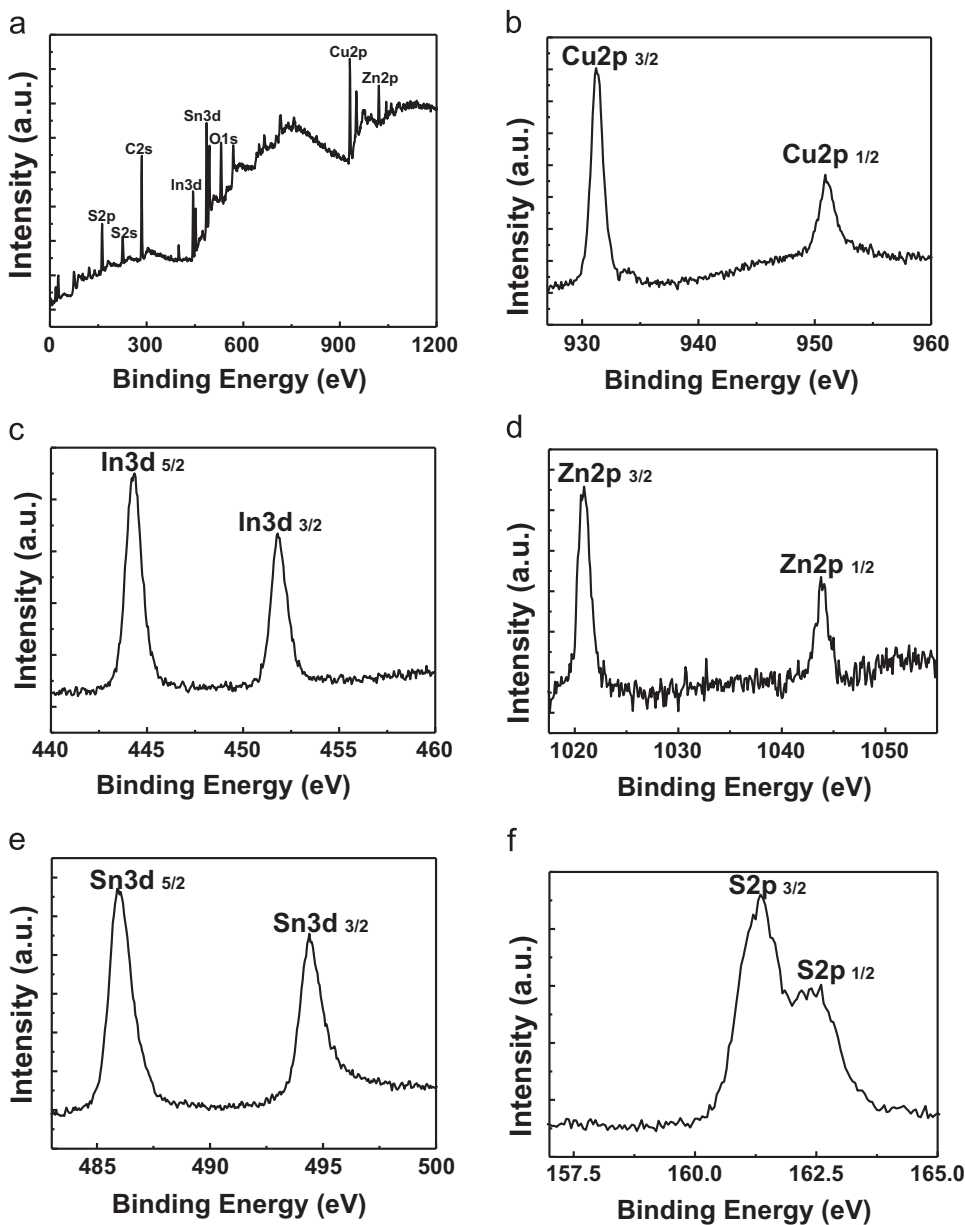


Fig. 2. (a) X-Ray Photoelectron Spectroscopy of $\text{Cu}_3\text{InZnSnS}_6$ nanocrystals; (b) $\text{Cu}2p$; (c) $\text{In}3d$; (d) $\text{Zn}2p$; (e) $\text{Sn}3d$; (f) $\text{S}2p$.

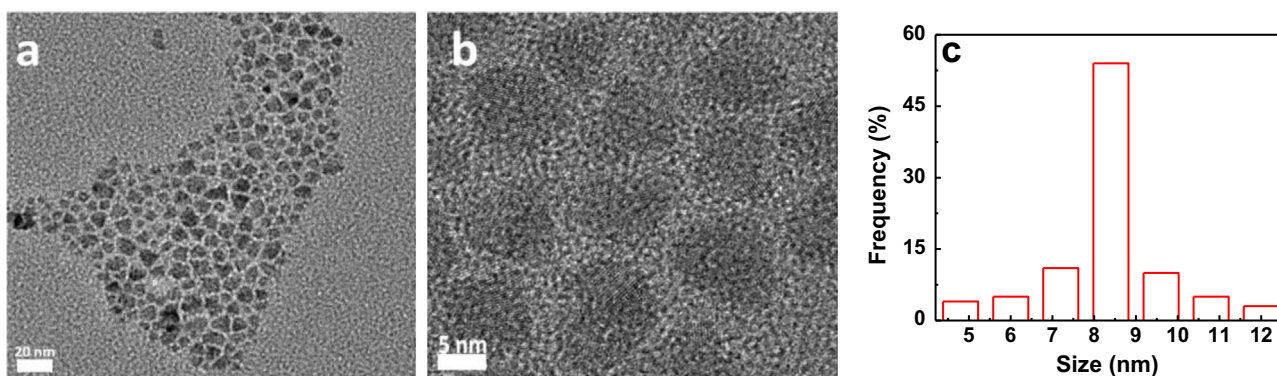


Fig. 3. TEM images of as-synthesized $\text{Cu}_3\text{InZnSnS}_6$ nanocrystals, (a) low resolution, (b) high resolution, (c) size distribution of $\text{Cu}_3\text{InZnSnS}_6$ nanocrystals.

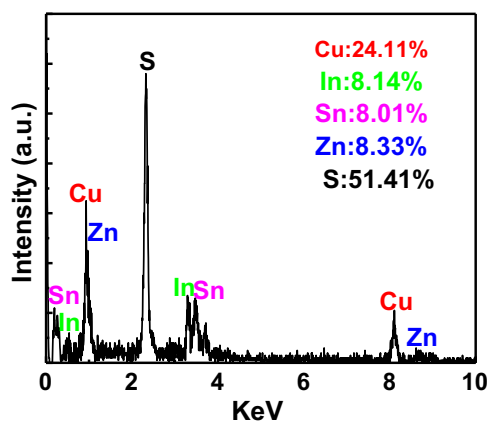


Fig. 4. EDS spectra of zincblende $\text{Cu}_3\text{InZnSnS}_6$ nanocrystals.

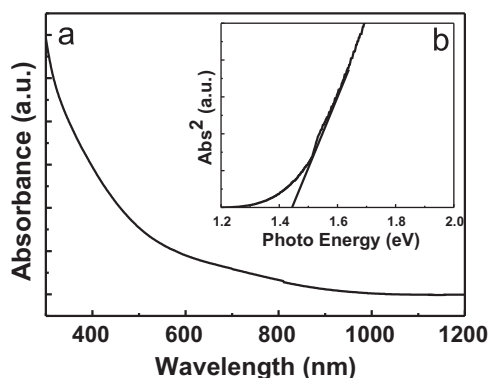


Fig. 5. (a) UV-vis-NIR absorption spectra of $\text{Cu}_3\text{InZnSnS}_6$ nanocrystals in toluene; (b) abs^2 vs eV for the $\text{Cu}_3\text{InZnSnS}_6$ nanocrystals.

2.3. Characterization

The powder XRD patterns were recorded using a Bruker D8 Focus X-ray diffractometer. The simulated $\text{Cu}_3\text{InZnSnS}_6$ powder XRD pattern was obtained by using Diamond 3.0 and CCDC Mercury 1.4.2 programs. UV-vis-NIR absorption spectrum was measured by Shimadzu UV-3600. Low resolution TEM (LR-TEM) image and High resolution TEM (HR-TEM) image were taken on a FEI Tecnai G2 F20 with an accelerating voltage of 100 kV and 200 kV. Energy Disperse Spectroscopy (EDS) spectrum was obtained by using a scanning electron microscope (Hitachi S-4800) equipped with a Bruker AXS XFlash detector 4010. X-ray photoelectron spectra (XPS) were measured with VG ESCALAB MK (VK Company,

UK) at room temperature by using a Mg $K\alpha$ X-ray source at 14 kV and 20 mA.

3. Results and discussion

In order to investigate the structure of as-synthesized nanocrystals, X-ray powder diffraction was employed. Because there is no XRD pattern of $\text{Cu}_3\text{InZnSnS}_6$ alloy, Diamond 3.0 and CCDC Mercury 1.4.2 programs were used to simulate XRD diffraction pattern of $\text{Cu}_3\text{InZnSnS}_6$ alloy. As can be seen in the Fig. 1, the as-synthesized $\text{Cu}_3\text{InZnSnS}_6$ nanocrystals display the zincblende structure, corresponding well with the simulated one. The unit cell dimensions of zincblende $\text{Cu}_3\text{InZnSnS}_6$ nanocrystals are $a=b=c=5.145 \text{ \AA}$. The major diffraction peaks exhibited at $2\theta=28.44^\circ$, 47.54° and 56.16° can be indexed to the (111), (220) and (311) planes of the zincblende crystal structure. CuInS_2 and $\text{Cu}_2\text{ZnSnS}_4$ possess zincblende phase, therefore $\text{Cu}_3\text{InZnSnS}_6$ zincblende nanocrystals, viewed as combination of CuInS_2 and $\text{Cu}_2\text{ZnSnS}_4$, can also be synthesized by rationally adjusting the reaction parameter. Here oleylamine was used as single ligand that can be well capped Cu^+ , In^{3+} , Zn^{2+} , Sn^{4+} and balance the reactivity of above cations under chemical reaction condition. Sulfur source also play a significant role during the process of zincblende structure synthesis. The low reactivity of oleylamine/sulfur is inclined to synthesize zincblende phase materials.

X-ray photoelectron spectroscopy (XPS) was one of the most useful technologies to characterize elemental valence of the compound. Fig. 2 displays the XPS patterns of $\text{Cu}_3\text{InZnSnS}_6$ zincblende nanocrystals. The separation peaks of Cu 2p are 931.2 eV and 951.1 eV, respectively, indicating that oleylamine capped Cu is +1. The peaks of In, Zn, Sn are located at 444.3 eV and 451.18 eV, 1021 eV and 1043.8 eV, 485.9 eV and 494.4 eV, respectively, shows that the electronic state of above element is +3, +2 and +4, which is consistent well with the reported literature [6,13]. The peaks of sulfur anion of the nanocrystals are 161.3 eV and 162.6 eV. The valence state of sulfur is -2.

Fig. 3 displays the transmission electron microscopy (TEM) images of $\text{Cu}_3\text{InZnSnS}_6$ nanocrystals. The as-synthesized nanocrystals were nearly monodispersed in organic solvent-toluene, and the average size of the nanocrystals is 8 nm in the high resolution TEM image. Due to the good dispersed property of oleylamine capped $\text{Cu}_3\text{InZnSnS}_6$ nanocrystals, the $\text{Cu}_3\text{InZnSnS}_6$ nanocrystals absorber layer can be fabricated by spincoating, roll to roll or printing approach.

As known, the optical property of semiconductor material can be greatly influenced by the composition, so energy dispersive X-ray spectrometry was used to characterize the elemental composition. In the Fig. 4, the result shows that elemental composition of $\text{Cu}_3\text{InZnSnS}_6$ nanocrystals is closed to chemical

stoichiometry-3:1:1:1:6, demonstrated that oleylamine can well balance the reactivity of metal cations.

UV-vis spectra that is an effective approach to investigate optical property of semiconductor materials, was used to characterize zincblende $\text{Cu}_3\text{InZnSnS}_6$ nanocrystals. As known, the zincblende $\text{Cu}_3\text{InZnSnS}_6$ nanocrystals can be considered as combination of CuInS_2 and $\text{Cu}_2\text{ZnSnS}_4$, therefore the bandgap of zincblende CuInS_2 is 1.45 eV, and for the same structure of $\text{Cu}_2\text{ZnSnS}_4$, the bandgap is approximately 1.64 eV. The onset point of UV-vis spectra for $\text{Cu}_3\text{InZnSnS}_6$ nanocrystals is 860 nm, corresponding to the 1.44 eV bandgap. The average size of as-synthesized $\text{Cu}_3\text{InZnSnS}_6$ nanocrystals is 8 nm, therefore the UV-vis spectra reflects the optical absorption of 8 nm $\text{Cu}_3\text{InZnSnS}_6$ nanocrystals. The bandgap of $\text{Cu}_3\text{InZnSnS}_6$ nanocrystals is lower than the CuInS_2 and $\text{Cu}_2\text{ZnSnS}_4$ of the same structure. According to the previous literature [15,16], the intrinsic cationic defect and phonon anharmonic sub-system can influence the optical bandgap of semiconductor materials. The bandgap of $\text{Cu}_3\text{InZnSnS}_6$ nanocrystals is closed to the optimal bandgap value (1.5 eV) of single junction thin film solar cells. The UV-vis result shows that the $\text{Cu}_3\text{InZnSnS}_6$ nanocrystals have a great potential application in the field of solar cells.

In summary, metastable zincblende $\text{Cu}_3\text{InZnSnS}_6$ nanocrystals has been successfully synthesized via a hot-injection approach. The as-synthesized $\text{Cu}_3\text{InZnSnS}_6$ nanocrystals have a metastable zincblende structure, and stoichiometric composition. Meanwhile, the as-synthesized $\text{Cu}_3\text{InZnSnS}_6$ nanocrystals possess good

dispersed property in organic solvent, and could fabricate nanocrystals thin films by spin-casting approach or roll to roll way. The suitable optical bandgap displays that they can potentially be applied as absorber layer in the thin film solar cells.

References

- [1] Chen XB, Shen SH, Guo LJ, Mao SS. *Chem Rev.* 2010;110:6503–7570.
- [2] Chen GY, Seo JW, Yang CH, Prasad PN. *Chem. Soc. Rev.* 2013;42:8304–38.
- [3] Talapin DV, Lee JS, Kovalenko VM, Shevchenko EV. *Chem. Rev.* 2010;110:389–458.
- [4] Kershaw SV, Susha AS, Rogach AL. *Chem. Soc. Rev.* 2013;42:3033–87.
- [5] Azimi H, Hou Y, Brabec CJ. *Energy Environ. Sci.* 2014;7:1829–49.
- [6] Pan DC, An LJ, Sun ZM, Hou W, Yang Y, Yang ZZ, Lu YF. *J. Am. Soc. Chem.* 2008;130:5620–1.
- [7] Cui Y, Wang G, Pan DC. *CrystEngComm.* 2013;15:10459–63.
- [8] Norako ME, Brutchey RL. *Chem. Mater.* 2010;22:1613–5.
- [9] Singh A, Geaney H, Laffir F, Ryan KM. *J. Am. Soc. Chem.* 2012;134:2910–3.
- [10] Zou Y, Su X, Jiang J. *J. Am. Soc. Chem.* 2013;135:18377–84.
- [11] Singh A, Coughlan C, Laffir F, Ryan KM. *J. ACS Nano* 2012;6:6977–83.
- [12] Hao ZM, Cui Y, Wang G. *Mater. Lett.* 2015;146:77–80.
- [13] Liu QH, Zhao ZC, Lin YH, Guo P, Li SJ, Pan DC, Ji XL. *Chem. Comm.* 2011;47:964–6.
- [14] Lu XT, Zhuang ZB, Peng Q, Li YD. *Chem. Comm.* 2011;47:3141–3.
- [15] Gorgut GP, Fedorchuk AO, Kityk IV, Sachanyuk VP, Olekseyuk ID, Parasyuk OV. *J. Cryst. Growth* 2011;324:212–6.
- [16] Davydyuk GE, Myronchuk GL, Kityk IV, Danyl'chuk SP, Bozhko VV, Parasyuk OV. *Opt. Mater.* 2011;33:1302–6.